Dyes and Pigments 84 (2009) 114–120

Contents lists available at ScienceDirect

Dyes and Pigments

journal homepage: www.elsevier.com/locate/dyepig

Novel ESIPT fluorescent benzazolyl-4-quinolones: Synthesis, spectroscopic characterization and photophysical properties

Gisele O.W. Lins, Leandra F. Campo*, Fabiano S. Rodembusch, Valter Stefani*

Universidade Federal do Rio Grande do Sul, Instituto de Química, Laboratório de Novos Materiais Orgânicos, Av. Bento Gonçalves 9500, CP15003, CEP 91501-970, Porto Alegre, RS, Brazil

ARTICLE INFO

Article history:
Received 19 March 2009
Received in revised form
9 July 2009
Accepted 14 July 2009
Available online 29 July 2009

Keywords:
Gould-Jacobs
Fluorescent nucleosides
Benzazoles
Quinolones
Fluorescence
Proton-Transfer

ABSTRACT

Two, novel, benzazolyl-quinolone heterocycles, fluorescent by virtue of intramolecular proton transfer mechanism in the excited state (ESIPT), were obtained using the Gould-Jacobs reaction. The intramolecular cyclization step in the preparation of the anilinomethylene malonate derivatives was carried out using polyphosphoric acid, heat transfer fluids (*Dowtherm A Fluid*, mineral oil and diphenyl ether) as well as tandem methodology, at temperatures ranging from 180 °C to 250 °C. Tandem methodology provided better yields and lower by-product formation. The synthesized quinolones were characterized using elemental analysis, IR, ^{13}C and ^{1}H NMR spectroscopy. Photophysical behaviour was studied using UV–Vis and steady-state fluorescence, both in solution and in solid state. The quinolones were fluorescent in solution in the orange-red region (500–800 nm), under UV radiation, and displayed a large Stokes shift (165–194 nm).

1. Introduction

Quinolone systems are well known substances with great therapeutic importance with respect to infectious diseases, particularly in the treatment of viral [1,2] and bacterial [3–5] infections. These compounds offer the potential ability to function as synthetic nucleoside analogue precursors. Since the discovery of penicillin, the development of novel synthetic or natural molecules with highly specific antibacterial properties has attracted great interest [6,7] in which context, oxo-quinolines have been the focus of attention [8–10]. To overcome the problem of the development of bacterial resistance to antibacterial compounds, novel quinolones with specific properties have been developed [11–18].

In contrast, benzazole heterocycle derivatives can display a large Stokes' shifted fluorescence [19] in the visible region (450–700 nm) coupled with high quantum yield (ϕ) and molar extinction coefficient values. Such dyes are fluorescent owing to an excited state intramolecular proton transfer (ESIPT) mechanism, this fundamental process having received considerable attention since its discovery some 50 or so years ago [20]. According to the ESIPT mechanism, the excited enol (E_1), which arises from light absorption by the fundamental enol (E_0), is quickly converted to an excited keto tautomer (K_1). Intramolecular proton transfer occurs when a molecule contains both an acidic and a basic site which, upon electronic excitation, experience enhanced acidity or basicity, respectively [21] The excited keto tautomer (K_1) decays, therby emitting fluorescence as the fundamental keto tautomer (K_0), and the initial enol form (E_0) is regenerated [22,23]. Since most ESIPT processes are reversible, these systems have found application as UV-light stabilizers [24,25], laser dyes [26], sensors [27], DNA probes [28,29], in drug delivery systems [30], hybrid materials [31] and also as fluorescent probes [32–35].

This work concerns the synthesis of two, novel, bifunctional, benzazolyl-quinolone heterocycles in which the quinolone nucleus was synthesized using Gould-Jacobs cyclization [36], by means of which, the appropriate aniline is reacted with dialkylalkoxymethylene malonate to provide the anilinomethylene malonate. Subsequent heating induces Gould-Jacobs cyclization to afford the corresponding benzazolyl-4-quinolones derivatives.

2. Experimental

2.1. Materials

Reagent grade o-aminophenol, o-aminothiophenol and 5-aminosalicylic acid (Aldrich) were used without purification. Polyphosphoric acid (PPA) was purchased from ACROS Chemicals. The

* Corresponding authors. Tel.: +55 51 3308 7206; fax: +55 51 3308 7304.
E-mail addresses: campo@iq.ufrgs.br (L.F. Campo), vstefani@iq.ufrgs.br (V. Stefani).

0143-7208/$ – see front matter © 2009 Published by Elsevier Ltd.
doi:10.1016/j.dyepig.2009.07.010

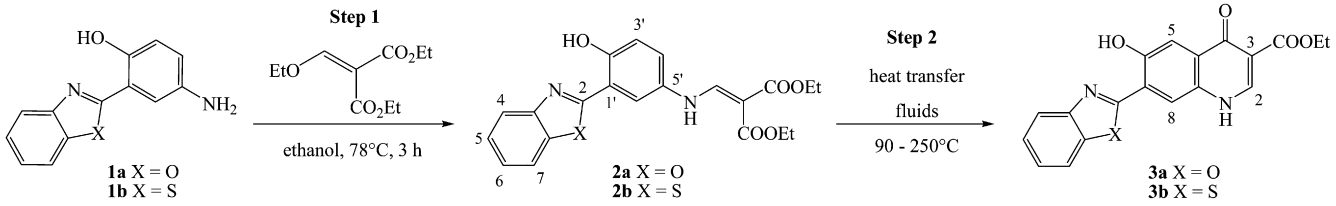

Fig. 1. Synthesis of the benzazolyl-4-quinolones.

diethyl(ethoxymethylene)malonate was purchased from Aldrich and used as received. *Dowtherm A* (Dow Chemicals Company), diphenyl ether (ACROS) and commercial mineral oil (Nujol) were used in the cyclization step. *Silicagel 60* (Merck) was used for chromatographic column separations. All solvents were used as received or were purified using standard procedures. Spectroscopic grade solvents (Merck) were used for the fluorescence and UV–Vis measurements.

2.2. Methods and instruments

Infrared spectra were recorded on a Mattson Galaxy Series FT-IR 3000 model 3020 in KBr pellets. Melting points were measured by dynamical scanning calorimetry using a Perkin–Elmer DSC-4 in a temperature range of 50–400 °C. Dry samples, 5–7 mg, were prepared in aluminum pan and sealed. The thermograms were obtained at a rate of 10 °C/min under nitrogen purge. ^{1}H and ^{13}C NMR spectra were performed on a VARIAN model VXR-200 or INOVA-300 using tetramethylsilane (TMS) as the internal standard and DMSO-d_6 (Aldrich) or $CDCl_3$ (Merck) as the solvent at room temperature. UV–Vis absorption spectra were performed on a Varian Cary 50 spectrophotometer. UV–Vis absorption data for fluorescence quantum yield were taken on a Shimadzu UV-1601 PC spectrophotometer. Fluorescence spectra were measured with a Hitachi spectrofluorometer model F-4500. Spectrum correction was performed to enable measuring a true spectrum by eliminating instrumental response such as wavelength characteristics of the monochromator or detector using Rhodamine B as a standard (quantum counter). The quantum yield of fluorescence (ϕ_{fl}) was made at 25 °C in spectroscopic grade solvents with a solution with absorbance intensity lower than 0.05. Quinine sulphate (Riedel) in H_2SO_4 1 M ($\phi_{fl} = 0.55$) was used as quantum yield standard [37]. Mass spectra were performed on a Hewlett–Packard 1100 MSD mass spectrometer (ESI-MS, APCI-MS) with positive mode.

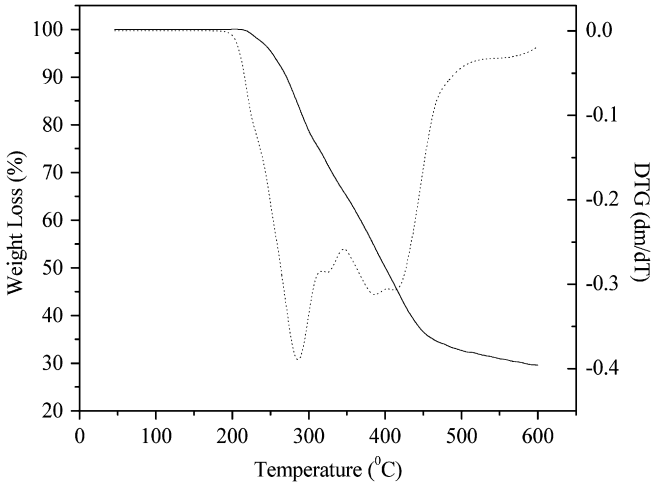

Fig. 2. TGA and DTG curves from the anilinomethylene malonate **2a**.

2.3. General procedure for the synthesis of the anilinomethylene malonates (**2a**–**b**)

The dyes **1a**–**b** and **2a**–**b** were obtained using the previously described method [32,38]. To a solution of the corresponding amino derivative **1a**–**b** in ethanol (40 ml) was added an equimolar amount of the diethyl (ethoxymethylene)malonate and the ensuing was heated at reflux for 3 h. The precipitate in the reaction mixture was filtered, washed with hot ethanol and dried at room temperature. The product was purified using column chromatography eluted with dichloromethane. In the tandem methodology, where several bonds are formed in sequence without isolating intermediates, changing reaction conditions, or adding reagents, the product was used without further purification.

2.3.1. 2-(5′-N-diethylmethylenemalonate-2′-hydroxyphenyl) benzoxazole (**2a**)

Yield: 78%. M.p.: 200–202 °C. Anal. Calcd for $C_{21}H_{20}N_2O_6$ (396.13 g mol^{-1}): C, 63.63; H, 5.09; N, 7.07. Found: C, 64.02; H, 4.73; N, 7.22. IR (cm^{-1}): ν = 3247 (NH), 3090 (C–H)$_{arom}$, 1700 (C═O), 1650 (C═C)$_{alif}$, 1230 (C–O–C). ^{1}H NMR (300 MHz, $CDCl_3$): δ (ppm) = 11.37 (s, 1H, OH); 11.10 (d, 1H, NH, J = 13.8 Hz); 8.50 (d, 1H, NCH, J = 13.8 Hz); 7.81 (d, 1H, $H_{6'}$, J = 2.8 Hz); 7.78–7.74 (m, 2H, H_4 or H_7); 7.66–7.63 (m, 2H, H_7 or H_4); 7.46–7.39 (m, 2H, H_5 and H_6); 7.23 (d, 1H, $H_{4'}$, J_m = 2.8 Hz, J_o = 8.9 Hz); 7.14 (d, 1H, $H_{3'}$, J_o = 8.9 Hz); 4.33 (q, 2H, CH_2); 4.28 (q, 2H, CH_2); 1.39 (t, 3H, CH_3) and 1.39–1.35 (t, 3H, CH_3). ^{13}C NMR (50 MHz, $CDCl_3$): δ (ppm) = 170, 167, 163, 157, 153, 150, 141, 133, 127, 126, 124, 121, 120, 116, 112 (2C), 112, 94, 62, 61, 16 (2C).

2.3.2. 2-(5′-N-diethylmethylenemalonate-2′-hydroxyphenyl) benzothiazole (**2b**)

Yield: 86%. M.p.: 164–167C. Anal. Calcd for $C_{21}H_{20}N_2O_5S$ (412.46 g mol^{-1}): C, 61.15; H, 4.89; N, 6.79. Found: C, 61.04; H, 5.38; N, 6.38. IR (cm^{-1}): ν = 3252 (NH), 3090 (C–H)$_{arom}$, 1700 (C═O), 1650 (C═C)$_{alif}$ and 1220 (C–O–C). ^{1}H NMR (200 MHz, $CDCl_3$): δ (ppm) = 12.42 (s, 1H, OH); 11.10 (d, 1H, NH, J = 13.4 Hz); 8.50 (d, 1H, NCH, J = 13.4 Hz); 7.97–7.87 (m, 2H, H_4 and H_7); 7.50–7.37 (m, 2H, H_5 and H_6); 7.32–7.31 (d, 1H, $H_{6'}$, J_m = 2.4 Hz); 7.20–7.18 and 7.14–7.13 (2d, $H_{4'}$, J_m = 2.4 Hz, J_o = 9.0 Hz); 7.10–7.05 (d, 1H, $H_{3'}$, J_o = 9.0 Hz); 4.32 (q, CH_2); 4.27 (q, CH_2); 1.40 (t, CH_3); 1.36 (t, CH_3). ^{13}C NMR (75.4 MHz, $CDCl_3$): δ (ppm) = 169, 168, 166, 155, 152, 151, 132, 131, 126–117 (7C), 93, 60 (2C) 14 (2C).

2.4. General procedure for the synthesis of the benzazolyl-4-quinolone dyes (**3a**–**b**)

Intramolecular cyclization was studied using polyphosphoric acid (Procedure 1), heat transfer fluids (Procedures 2–4) as well as tandem methodology (Procedure 5).

Procedure 1: A solution of the anilinomethylene malonate (**2a** or **2b**) in polyphosphoric acid (1:10 w/w) was heated at 180 °C for 1 h under N_2 atmosphere; the reaction was monitored by TLC using chloroform as eluent. The expected quinolone could not be obtained.

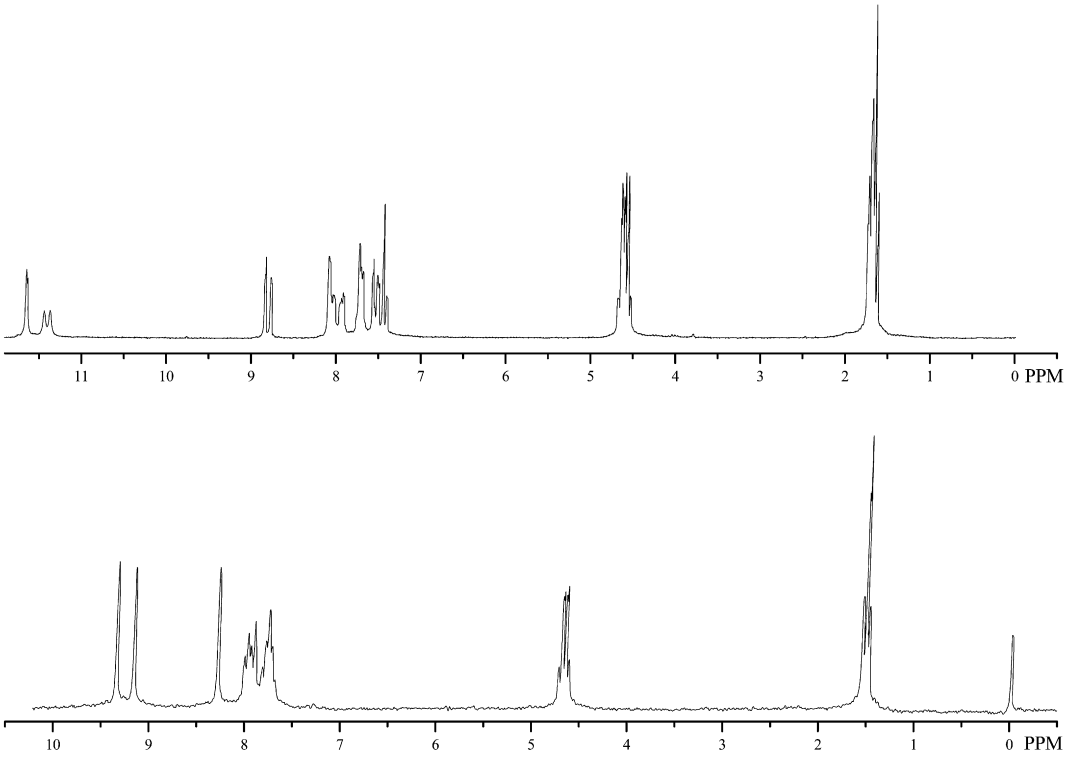

Fig. 3. ^{1}H NMR spectra from the malonate **2a** (top) and quinolone **3a** (bottom).

Procedure 2: A solution of the anilinomethylene malonate (**2a** or **2b)** (2.52 mmol) in *Dowtherm A* (20 ml) was heated at 250 °C for 2 h under N_2 atmosphere; the reaction was monitored by TLC using chloroform as eluent. The reaction mixture was filtered, washed several times with hexane, petroleum ether and chloroform and dried at 60 °C. Yield: 8% (**3a**) and 9% (**3b**).

Procedure 3: A solution of the anilinomethylene malonate (**2a** or **2b)** (2.52 mmol) in *Nujol* (20 ml) was heated at 250 °C for 2 h under N_2 atmosphere; the reaction was monitored by TLC using dichloromethane/acetone (10:1) as eluent. The reaction mixture was filtered, washed several times with hexane, petroleum ether and chloroform and dried at 60 °C. Yield: 10% (**3a**) and 5% (**3b**).

Procedure 4: The anilinomethylene malonate (**2a** or **2b)** (1.54 mmol) were slowly added to the diphenyl ether at 230 °C and kept to react for 3 h under N_2 atmosphere. The reaction was monitored by TLC using dichloromethane/acetone (4:1) as eluent. After cooling at room temperature, the reaction mixture was filtered, washed several times with hexane, petroleum ether and chloroform and dried at 60 °C. Yield: 13% (**3a**) and 7% (**3b**).

Procedure 5: An equimolar amount of the amino benzazole (**1a** or **1b)** (2.23 mmol) and diethyl (ethoxymethylene)malonate in diphenyl ether (6 ml) was heated at 80 °C for 30 min under a N_2 atmosphere. In this reaction step, the *N*-ethylene derivatives (**2a** or **2b**) were identified by TLC using dichloromethane as eluent and were used in the subsequent cyclization step without isolation. The temperature was increased to 230 °C and reaction continued for 3–4 h; the reaction was monitored by TLC using chloroform/acetone (10:1) as eluent. After cooling at room temperature, hexane was added to precipitate the product, which was filtered and then washed several times with hexane and chloroform. The product was purified by recrystallization in DMF. The crystallized product was washed with acetone and dried at 60 °C. Yield: 15% (**3a**) and 10% (**3b**).

*2.4.1. Ethyl 7-(benzoxazol-2-yl)-1,4-dihydro-6-hydroxy-4-quinolone-3-carboxylate (**3a**)*

M.p.: 350 °C. Anal. Calcd for $C_{19}H_{14}N_2O_5$ (350.09 g mol^{-1}): C, 65.14; H, 4.03; N, 8.00. Found: C, 65.04; H, 3.91; N, 7.85. IR (cm^{-1}): ν = 3145 (NH), 3105 (OH), 2975 (C–H)$_{arom}$, 1691 (C═O), 1612 (C═O), 1552 (C═C)$_{alif}$, 1176 (C–O–C). ^{1}H NMR (200 MHz, $CDCl_3$+CF_3COOH): δ (ppm) = 9.32 (s, H_5); 9.14 (s, H_8); 8.27 (s, H_2); 8.01–7.70 (m, 4H); 4.60–4.71 (q, CH_2); 1.48–1.55 (t, CH_3). ^{13}C NMR (50 MHz, $CDCl_3$+CF_3COOH): δ (ppm) = 173, 168, 160 (C═O ester), 157, 150, 147, 134, 132, 131, 130, 127, 125, 118, 117, 114, 112, 105, 66, 14. Relation *m*/*z* in Da(%) = 63(14); 152(11); 192(11); 219(18); 248(6); 276(6); 304(100); 350 (M^+, 27). The molecular mass for $C_{19}H_{14}N_2O_5$ *m*/*z* = 350.09 Da was confirmed by MS.

*2.4.2. Ethyl 7-(benzothiazol-2-yl)-1,4-dihydro-6-hydroxy-4-quinolone-3-carboxylate (**3b**)*

M.p.: 334 °C. Anal. Calcd for $C_{19}H_{14}N_2O_4S$ (366.07 g mol^{-1}): C, 62.28; H, 3.85; N, 7.65. Found: C, 61.94; H, 3.72; N, 7.77. IR (cm^{-1}): ν = 3118 (NH), 3068 (OH), 2983 (C–H)$_{arom}$, 1701 (C═O), 1610 (C═O), 1552 (C═C)$_{alif}$, 1189 (C–O–C). ^{1}H NMR (200 MHz, $CDCl_3$+CF_3COOH): δ (ppm) = 9.33 (s, H_5); 9.08 (s, H_8); 8.35 (s, H_2); 7.98–7.91 (m, 2H); 8.33–8.28 (m, 2H); 4.62–4.72 (q, CH_2); 1.49–1.56 (t, CH_3). ^{13}C NMR (50 MHz, $CDCl_3$+CF_3COOH): δ (ppm) = 171, 170, 158 (C═O ester), 157, 151, 149, 132, 130, 131, 130, 128, 125, 117, 116, 113, 112, 103, 66, 14. Relation *m*/*z* in Da(%) = 69(15); 109(12); 184(10); 209(21); 237(25); 292(18); 320(100); 366 (M^+, 27). The molecular mass for $C_{19}H_{14}N_2O_4S$ *m*/*z* = 366.07 Da was confirmed by MS.

3. Results and discussion

3.1. Synthesis of the benzazolyl-4-quinolones

The benzazolyl-4-quinolones (**3a**–**b**) were obtained using a two-step synthesis (Fig. 1) namely, initial nucleophilic attack on diethyl(ethoxymethylene)malonate (Step 1) to produce the

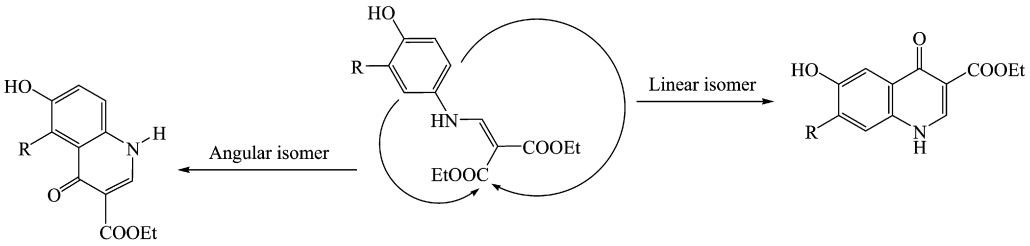

Fig. 4. Cyclization angular and linear anilinomethylene malonates, where R is benzaxolyl or benzothiazolyl.

anilinomethylene malonates (**2a**–**b**) [15] followed by intramolecular cyclization (Step 2). This final step was studied using polyphosphoric acid, heat transfer fluids and tandem methodology.

Although polyphosphoric acid has already been used in quinolone synthesis [36,39] it was not be possible to obtain the desired benzazolyl-4-quinolones, most likely due to the nitrogen protonation of the anilinomethylene malonate (**2a**–**b**), which deactivated the aromatic ring in the intramolecular cyclization step [13]. The use of heat transfer fluids (*Dowtherm A*, diphenyl ether and commercial mineral oil) at high temperature allowed the formation of the products **3a**–**b** with a large amount of by-products formation. Since the cyclization step is characterized by loss of an ethanol molecule, attempts were performed in order to optimize the intramolecular cyclization temperature, by means of thermogravimetric study of the anilinomethylene malonate. Fig. 2 depicts the thermogravimetric curve of the malonate **2a**. Similar thermogravimetric behaviour was detected for the benzothiazolyl analogue. It is of note that the cyclization step was performed using an open flask to permit ethanol evaporation so as to expedite product yield.

Although an additional methodology using Eaton's Reagent was employed in order to improve the yield of the benzazolyl-4-quinolone [40], yields (∼2%) were lower than those presented in this paper.

Despite the five-step degradation processes observed in the malonate **2a**, a thermal degradation process related to a mass loss of 13% (ethanol molecule) can be observed between 219 and 285 °C. The observed thermal behaviour, which is characterized by many degradation steps, probably indicates by-product formation, which is related to the low yield of **3a**–**b**. In this way, the cyclization step using diphenyl ether was performed between 210 and 230 °C and showed to be the best reaction condition to obtain the quinolones, since the by-product formation was minimized and the products could be easily isolated.

A tandem methodology was also studied using diphenyl ether as solvent, which proved to be the best heat transfer fluid for the Gould-Jacobs cyclization employed herein. The anilinomethylene malonates (**2a**–**b**) were obtained from the aminobenzazoles (**1a**–**b**) and the diethyl(ethoxymethylene)malonate. The reaction was monitored by TLC. The temperature was increased to allow the intramolecular cyclization when the starting materials (**1a**–**b**) could not be detected by TLC. It is of note that the benzimidazole derivative was obtained in very low crude yield in relation to the O and S analogues and its reaction presented many by-products. This product could not be characterized.

3.2. Spectroscopic characterization

Fig. 3 presents the ^{1}H NMR spectra of the heterocycles **2a** (top) and **3a** (bottom). Due to the low solubility of the quinolones, the spectra were performed using a mixture of $CDCl_3/CF_3COOH$. The structural changes of the anilinomethylene malonates after the cyclization step can be clearly observed by NMR spectroscopy. The signal splitting between the enaminic and olefinic protons present in **2a** (J = 13.8 Hz) and **2b** (J = 13.4 Hz) at 11.10 ppm is not observed in the quinolones **3a**–**b** (only a single signal at 11.10 ppm). The olefinic proton, which can be observed as a doublet in the malonates (8.50 ppm) after cyclization, appears as a singlet (8.27 ppm to **3a** and 8.35 ppm to **3b**). This change is related to the bond constraints between the olefinic carbon and enamine nitrogen after

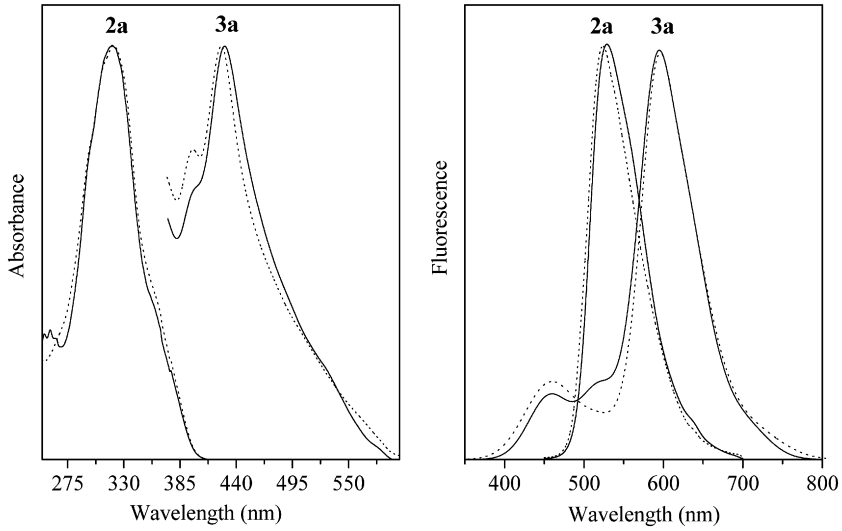

Fig. 5. Normalized UV–Vis absorption and fluorescence emission spectra of the anilinomethylene malonate **2a** and its respective quinolone **3a** in chloroform (solid line) and dioxane (dot line).

Table 1
UV–Vis absorption and fluorescence emission data in chloroform and dioxane. The Stokes shifts ($\Delta\lambda_{ST}$) are presented in nanometers and the molar extinction coefficient values (ε_{max}) are presented in $lmol^{-1}cm^{-1}$.

Dye	Solvent	λ_{max}^{abs}(nm)	ε_{max} x10^{-4}	λ_{max}^{em}(nm)	$\Delta\lambda_{ST}$	ϕ_{fl}
2a	Chloroform	318	3.1	529	211	0.20 [38]
	Dioxane	320	4.5	523	203	0.17
2b	Chloroform	321	3.6	569	248	0.41 [38]
	Dioxane	321	3.3	562	241	0.38
3a	Chloroform	429	4.5	594	165	0.15
	Dioxane	425	3.9	597	172	0.13
3b	Chloroform	442	3.0	635	193	0.25
	Dioxane	444	4.2	638	194	0.22

cyclization. Note that the ethyl moiety from each malonate appears as four different signals (two triplets and two doublets). After cyclization, only one triplet and one doublet can be seen in the aliphatic region, which indicates the loss of an ethyl moiety, as expected. Additionally, no coupling could be observed between the protons H_5 and H_8 in the aromatic region, which indicates a cyclization in *meta* position toward the hydroxyl group to produce the linear isomer (Fig. 4). The ABX system present in the malonate also can not be observed due to the loss of the proton $H_{4'}$ to form two singlets related to protons H_5 and H_8 located over 9 ppm.

3.3. Photophysical characterization

Figs. 5 and 6 show the normalized UV–Vis absorption and fluorescence emission spectra of the quinolones **3a**–**b** and the respective malonates **2a**–**b**. The curves were obtained in chloroform and dioxane and using the absorption maxima as the excitation wavelengths. The relevant UV–Vis and fluorescence data are summarized in Table 1.

An absorption maxima bands located around 318–320 nm, with molar extinction coefficient values (ε_{max}) in agreement with π–π^* transitions, could be observed in the malonate **2a**. Usually, in azole heterocycles, the nonbonding electrons from the oxygen or sulfur and the nitrogen interacts each other increasing the gap to the $n\rightarrow\pi^*$ transition. On the other hand, its planar structure decreases the energy to the $\pi\rightarrow\pi^*$. In this way, the absorption band maxima is due to the phenolic ring orbital (HOMO) to the azolic empty orbital (LUMO), which results to an allowed transition $\pi\rightarrow\pi^*$ with higher values to the molar extinction coefficient, as observed. A red shift, higher than 100 nm, could be observed in the absorption maxima of the quinolone **3a** (429 nm in chloroform and 425 nm in dioxane) in relation on its precursor, which can be related to a more conjugate structure after cyclization, as expected. The quinolone **3a** presents in chloroform and dioxane two fluorescence emission bands. A main band located at around 594–597 nm related to the ESIPT mechanism and a small one, blue shifted, located at 458–460 nm, ascribed to the normal emission [19]. A large Stokes shift values (165 and 172 nm) could be observed in the quinolone **3a**.

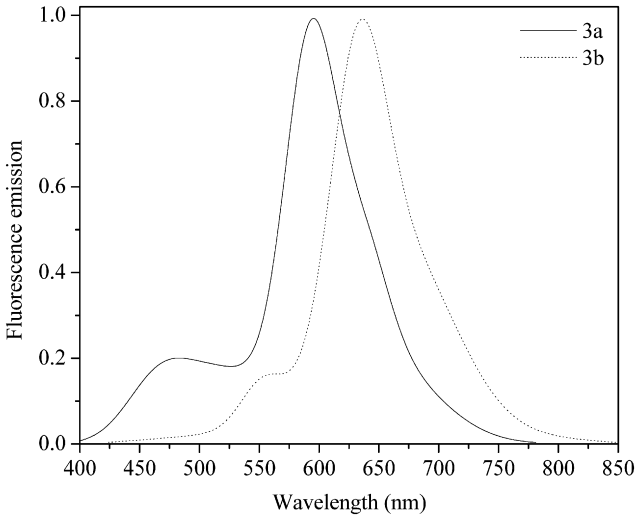

Fig. 7. Normalized fluorescence emission spectra in the solid state.

A similar photophysical behavior was observed in the malonate **2b** and its quinolone **3b** (Fig. 6) if compared to the oxazole analogues. An absorption maxima located at around 321 nm and 442–444 nm to **2b** and **3b** respectively, with molar extinction coefficient values in agreement with $\pi\rightarrow\pi^*$ transitions. However, the red shift was higher than observed to **2b** (>120 nm), which can be explained by the better electron delocalization allowed by the sulfur atom in relation to the oxygen [19]. The quinolone **3b**

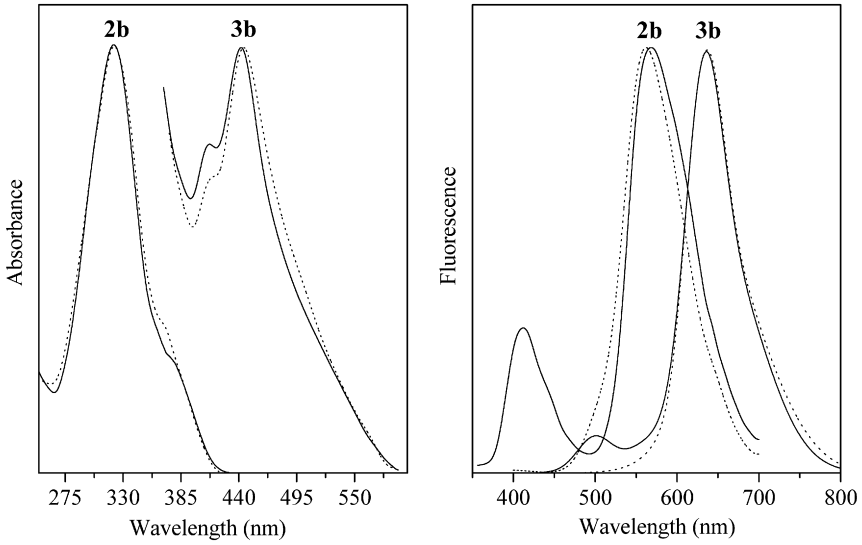

Fig. 6. Normalized UV–Vis absorption and fluorescence emission spectra of the anilinomethylene malonate **2b** and its respective quinolone 3b in chloroform (solid line) and dioxane (dot line).

Fig. 8. Quinolones 3a–b under visible light (top) and UV radiation (bottom), where in solution (left): (a) dye 3a in chloroform, (b) dye 3a in dioxane, (c) dye 3b in chloroform and (d) dye 3b in dioxane, and in the solid state (right).

presents in dioxane one main band located at 638 nm (ESIPT band). A dual fluorescence emission, as already observed in the oxazole analogue **3a**, could be observed. The main fluorescence band located at 635 nm and the blue shifted one located at 500 nm. The quinolone **3b** also presented large Stokes shift values (193–194 nm), which is expected when a tautomerism takes place in the excited state [19].

Fig. 7 shows the normalized fluorescence emission spectra in the solid state of the quinolones **3a**–**b**. Although molecules which undergo excited state intramolecular proton-transfer present sensitivity to the surrounding medium [19], the obtained quinolones showed that the solvents do not play a fundamental role on its photophysics. A similar behaviour could be detected in solution and in the solid state, with a main band located at 596 nm (594 nm in solution) and 636 nm (638 nm in solution) to the quinolones **3a** and **3b**, respectively. Fig. 8 depicts the quinolones in solution (left) and in the solid state (right), under visible light (top) and UV radiation (bottom).

4. Conclusions

Two new benzazolyl-4-quinolones, fluorescent by an intramolecular proton transfer mechanism in the excited state (ESIPT), were synthesized by cyclization of anilinomethylene malonates. The tandem methodology showed the best results, presenting better yields and lower by-products formation. It could not be possible to obtain a quinolone derivative from the benzimidazole derivative. The obtained products were fully characterized and present fluorescence emission in the orange-red region (594–637 nm) with a large Stokes shift (167–194 nm). Despite the low yields, the observed photophysical characteristics of these benzazole derivatives, such as the photostability and high Stokes shift, are very valuable, giving rise to potential applications as chemosensors [41–44].

Acknowledgments

We are grateful for financial support and scholarships from the Brazilian agencies CNPq, CAPES and FAPERGS.

References

[1] Wang ZQ, Vince R. Synthesis of pyrimidine and quinolone conjugates as a scaffold for dual inhibitors of HIV reverse transcriptase and integrase. Bioorganic & Medicinal Chemistry Letters 2008;18:1293–6.
[2] Fujita M, Egawa H, Chiba K, Matsumoto J. One-step furan ring formation: synthesis of furo[3,2-h]quinolones. Heterocyclic Chemistry 1997;34:1731–5.
[3] Patrick GL, editor. An introduction to medicinal chemistry. New York: Oxford University Press; 1995. p. 336.
[4] Dax SL, editor. Antibacterial chemotherapeutic agents. Pennsylvania: Springer; 1997. p. 298.
[5] Mitscher LA. Bacterial topoisomerase inhibitors: quinolone and pyridone antibacterial agents. Chemical Reviews 2005;105:559–92.
[6] Leyva E, Monreal E, Hernández A. Synthesis of fluoro-4-hydroxyquinoline-3-carboxylic acids by the Gould–Jacobs reaction. Journal of Fluorine Chemistry 1999;9:7–10.
[7] Bhanot SK, Singh M, Chatterjee NR. The chemical and biological aspects of fluoroquinolones: reality and dreams. Current Pharmaceutical Design 2001; 7:311–35.
[8] de Souza MVN, de Almeida MV. Drugs anti-HIV: past, present and future perspectives. Química Nova 2003;26:366–72.
[9] da Silva AD, de Almeida MV, de Souza MVN, Couri MRC. Biological activity and synthetic metodologies for the preparation of fluoroquinolones, a class of potent antibacterial agents. Current Medicinal Chemistry 2003;10:21–39.
[10] (a) Farhanullah Kim SY, Yoon EJ, Xu GY, Choi EC, Kim S, Kang T, et al. Design and synthesis of quinolinones as methionyl-tRNA synthetase inhibitors. Bioorganic & Medicinal Chemistry 2006;14:7154–9;
(b) Zhao GY, Miller MJ, Franzblau S, Wan B, Möllmann U. Syntheses and studies of quinolone-cephalosporins as potential anti-tuberculosis agents. Bioorganic & Medicinal Chemistry Letters 2006;16:5534–7.
[11] Srivastava BK, Solanki M, Mishra B, Soni R, Jayadev S, Valani D, et al. Synthesis and antibacterial activity of 4,5,6,7-tetrahydro-thieno[3,2-c]pyridine quinolones. Bioorganic & Medicinal Chemistry Letters 2007;17:1924–9.
[12] Winter RW, Kelly JX, Smilkstein MJ, Dodean R, Hinrichs D, Riscoe MK. Antimalarial quinolones: synthesis, potency, and mechanistic studies. Experimental Parasitology 2008;118:487–97.
[13] Mullock EB, Searby R. Synthetic uses of polyphosphoric acid and its ethyl ester. 2. Syntheses of indolin-2(3h)-ones and imidazoquinolines. Journal of the Chemical Society C: Organic 1970:829–33.
[14] Milata V. Alkoxymethylenemalonates in organic synthesis. Aldrichimica Acta 2001;34:20–7.
[15] Salon J, Milata V, Gatial A, Prónayová N, Lesko J, Cernuchová P, et al. Nucleophilic vinylic substitution (SNV) of activated alkoxymethylene derivatives with 6-aminoquinoxaline. European Journal of Organic Chemistry 2005;22:4870–8.
[16] Brosius R, Gammon D, van Laar F, van Steen E, Sels B, Jacobs P. Vapour-phase synthesis of 2-methyl- and 4-methylquinoline over BEA zeolites. Journal of Catalysis 2006;239:362–8.
[17] Stern E, Millet R, Depreux P, Hénichart JP. A versatile and efficient synthesis of 3-aroyl-1,4-dihydroquinolin-4-ones. Tetrahedron Letters 2004;45:9257–9.

[18] Hirano J, Hamase K, Zaitsu K. Evaluation of a simple and novel fluorescent anion sensor, 4-quinolone, and modification of the emission color by substitutions based on molecular orbital calculations. Tetrahedron 2006;62:10065–71.
[19] Rodembusch FS, Campo LF, Leusin FP, Stefani V. Excited state intramolecular proton transfer in amino 2-(2′-hydroxyphenyl)benzazole derivatives. Effects of the solvent and the amino group position. Journal of Luminescence 2007; 126:728–34.
[20] Weller A. Innermolekularer protonenubergang im angeregten zustand. Zeitschrift Fur Elektrochemie 1956;60(9–10):1144–7.
[21] Ireland JF, Wyatt PAH. Acid–base properties of electronically excited states of organic molecules. Advances in Physical Organic Chemistry 1976;12:131–221.
[22] Acuña AU, Amat F, Catalán J, Costela A, Figuera LM, Muños JM. Pulsed liquid-lasers from proton-transfer in the excited-state. Chemical Physics Letters 1986;132:567–9.
[23] Acuña AU, Costela A, Muños JM. A proton-transfer laser. Journal of Physical Chemistry 1986;90:2807–8.
[24] Catalán J, Fabero F, Guijarro MS, Claramunt RM, Santa Maria MD, Foces-Foces MC, et al. Photoinduced intramolecular proton-transfer as the mechanism of ultraviolet stabilizers. A reappraisal. Journal of the American Chemical Society 1990;112:747–59.
[25] Kuila D, Kvakovszky G, Murphy MA, Vicari R, Rood MH, Fritch KA, et al. Tris(hydroxyphenyl)ethane benzotriazole: a copolymerizable UV light stabilizer. Chemistry of Materials 1999;11:109–16.
[26] Uzhinov BM, Druzhinin SI. Excited state proton transfer lasers. Russian Chemical Reviews 1998;67:123–36.
[27] (a) Tong H, Zhou G, Wang L, Jing X, Wang F, Zhang J. Novel highly selective anion chemosensors based on 2,5-bis(2-hydroxyphenyl)-1,3,4-oxadiazole. Tetrahedron Letters 2003;44:131–4;
(b) Klymchenko AS, Demchenko AP. Electrochromic modulation of excited-state intramolecular proton transfer: the new principle in design of fluorescence sensors. Journal of the American Chemical Society 2002;124:12372–9;
(c) Shynkar VV, Klymchenko AS, Piemont E, Demchenko EP, Mely Y. Dynamics of intermolecular hydrogen bonds in the excited states of 4′-dialkylamino-3-hydroxyflavones. On the pathway to an ideal fluorescent hydrogen bonding sensor. Journal of Physical Chemistry A 2004;108:8151–9.
[28] Abella CAM, Rodembusch FS, Stefani V. Synthesis of novel Tröger's bases analogues. The first ones fluorescent by excited state intramolecular proton transfer (ESIPT). Tetrahedron Letters 2004;45:5601–4.
[29] Abou-Zied OK, Jimenez R, Romesberg FE. Tautomerization dynamics of a model base pair in DNA. Journal of the American Chemical Society 2001; 123:4613–4.
[30] Jager A, Stefani V, Guterres SS, Pohlmann AR. Physico-chemical characterization of nanocapsule polymeric wall using fluorescent benzazole probes. International Journal of Pharmaceutics 2007;338:297–305.
[31] (a) Kober UA, Campo LF, Costa TMH, Stefani V, Ramminger GD, Gallas MR. Fluorescence behavior of powders and high-pressure compacts of silica containing benzazole silyl-functionalized dyes. Journal of Photochemistry and Photobiology A: Chemistry 2007;186:24–8;
(b) Rodembusch FS, Campo LF, Rigacci A, Stefani V. A new ESIPT fluorescent dye-doped silica aerogel. Macromolecular Symposia 2005;229:188–93;
(c) Rodembusch FS, Campo LF, Rigacci A, Stefani V. The first silica aerogels fluorescent by excited state intramolecular proton transfer mechanism (ESIPT). Journal of Materials Chemistry 2005;15:1537–41.
[32] Holler MG, Campo LF, Brandelli A, Stefani V. Synthesis and spectroscopic characterization of 2-(2′-hydroxyphenyl)benzazole isothiocyanates as new fluorescent probes for proteins. Journal of Photochemistry and Photobiology A: Chemistry 2002;149:217–25.
[33] Rodembusch FS, Leusin FP, Medina LFC, Brandelli A, Stefani V. Synthesis and spectroscopic characterization of new ESIPT fluorescent protein probes. Photochemical & Photobiological Sciences 2005;4:254–9.
[34] Cardoso MB, Samios D, Silveira NP, Rodembusch FS, Stefani V. ESIPT-exhibiting protein probes: a more sensitive alternative to the biuret colorimetric test in the rice proteins detection. Photochemical & Photobiological Sciences 2007;6:99–102.
[35] Guzow K, Szabelski M, Malicka J, Karolczak J, Wiczk W. Synthesis and photophysical properties of 3-[2-(pyridyl)benzoxazol-5-yl]-L-alanine derivatives. Tetrahedron 2002;58:2201–9.
[36] Gould RG, Jacobs WA. The synthesis of certain substituted quinolines and 5,6-benzoquinolines. Journal of the American Chemical Society 1939;61:2890–5 [(and references cited therein)].
[37] Fery-Forgues S, Lavabre D. Are fluorescence quantum yields so tricky to measure? A demonstration using familiar stationery products. Journal of Chemical Education 1999;76:1260–4.
[38] Campo LF, Correa DS, de Araújo MA, Stefani V. New fluorescent monomers and polymers displaying an intramolecular proton transfer mechanism in the electronically excited state (ESIPT). Part I. synthesis of benzazolylvinilene derivatives and its copolymerization with PMMA. Macromolecular Rapid Communications 2000;21:832–6.
[39] Staskun B. New synthesis of 2-aryl-3-acetyl-4-hydroxyquinolines using polyphosphoric acid. Journal of Organic Chemistry 1961;69:2791–4.
[40] Zewge D, Chen CY, Deer C, Dormer PG, Hughes DL. A mild and efficient synthesis of 4-quinolones and quinolone heterocycles. Journal of Organic Chemistry 2007;72:4276–9.
[41] Polishchuk AV, Karaseva ET, Korpela T, Karasev VE. New luminophor-activators based on (fluoro)quinolone antibacterials. Journal of Luminescence 2008; 128:1753–7.
[42] Hirano J, Miyata H, Hamase K, Zaitsu K. A ratiometric fluorescent chemosensor, 1,10-phenanthroline-4,7-dione, for anions in aqueous-organic media. Tetrahedron Letters 2007;48:4861–4.
[43] Chen Y, Chi Y, Wen H, Lu Z. Sensitized luminescent terbium nanoparticles: preparation and time-resolved fluorescence assay for DNA. Analytical Chemistry 2007;79:960–5.
[44] Wang Y, Feng L, Jiang C. Fluorimetric study of the interaction between human serum albumin and quinolones–terbium complex and its application. Spectrochimica Acta A 2005;61:2909–14.